Available online at www.worldscientificnews.com

World Scientific News

WSN 45(2) (2016) 355-372 EISSN 2392-2192

Transmitter Inclination Angle Characteristics for Underwater Optical Wireless Communication in a Variety of APD Detectors

Mazin Ali A. Ali

Physics Department, College of Science, AL-Mustansiriyah University, Baghdad, Iraq

E-mail address: mazin79phy@yahoo.com

ABSTRACT

In this paper, the performance of an underwater optical wireless communications system is theoretically analyzed, using 4-PPM modulation technique and an avalanche photodiodes APD receiver over underwater environment channels. Based on the line of sight (LOS) geometrical model for optical beam propagation horizontally on an underwater medium and combined with signal to noise ratio model for Si, Ge and InGaAs APD and BER; then the impacts of the distance of transmission, power of the transmitter under Jerlov water types (I, IA, IB) are analyzed. The characteristics of bit error rate BER and channel capacity for 4-PPM optical modulation technique are studied under different APD detector and Jerlov water types. Simulation results indicate that the performance of PPM and Jerlov type (I) are more suited for an underwater optical wireless communication. On the other hand, we discuss the suitability of avalanche photodiodes under this modulation technique, where the photodiode Si APD has more advantage compared with the other detectors when used as a receiver in an underwater optical communication.

***Keywords*:** Communications; Underwater Optical Communications; Avalanche Photodiode; Bit Error Rate; Channel Capacity

1. INTRODUCTION

As the field of optical sources and photo-detector technology advances, communication through an underwater wireless optical channel (UWOC) has received a surge of attention by the researchers and scientists for wider bandwidth and higher data rate. UWOC fulfils several applications like underwater sensor networks (UWSNs), military applications, node-to- node communication, seismic activity sensing, and study of submarine life [1]. The large information bandwidth available at visible wavelengths has also opened the possibility for high-speed, wireless communications in an underwater environment. Unfortunately, the propagation of light underwater is affected by both absorption and scattering [2]. As a matter of fact, underwater wireless optical communication (UOWC) uses the visible band of the electromagnetic spectrum (the spectrum range of 450-550 nm), where water is relatively transparent to light and absorption takes its minimum value [3]. The attenuation coefficient indicates $c(\lambda)$ the total effects of absorption $\alpha(\lambda)$ and scattering on energy loss $\beta(\lambda)$ are shown in Fig. (1) [4]. The values of $c(\lambda)$ depend on both the wavelength λ as well as turbidity of water [5]. Most of the recent works [6,7], mainly concentrate on line of sight UWOC. But it adds more complexity, when it comes to implementation because of the obstructions in sea water. Line of Sight offers many advantages like, high data rate, no RF license, no security upgrade, immune to RF interference, low power, and increase in system bandwidth [8-11].

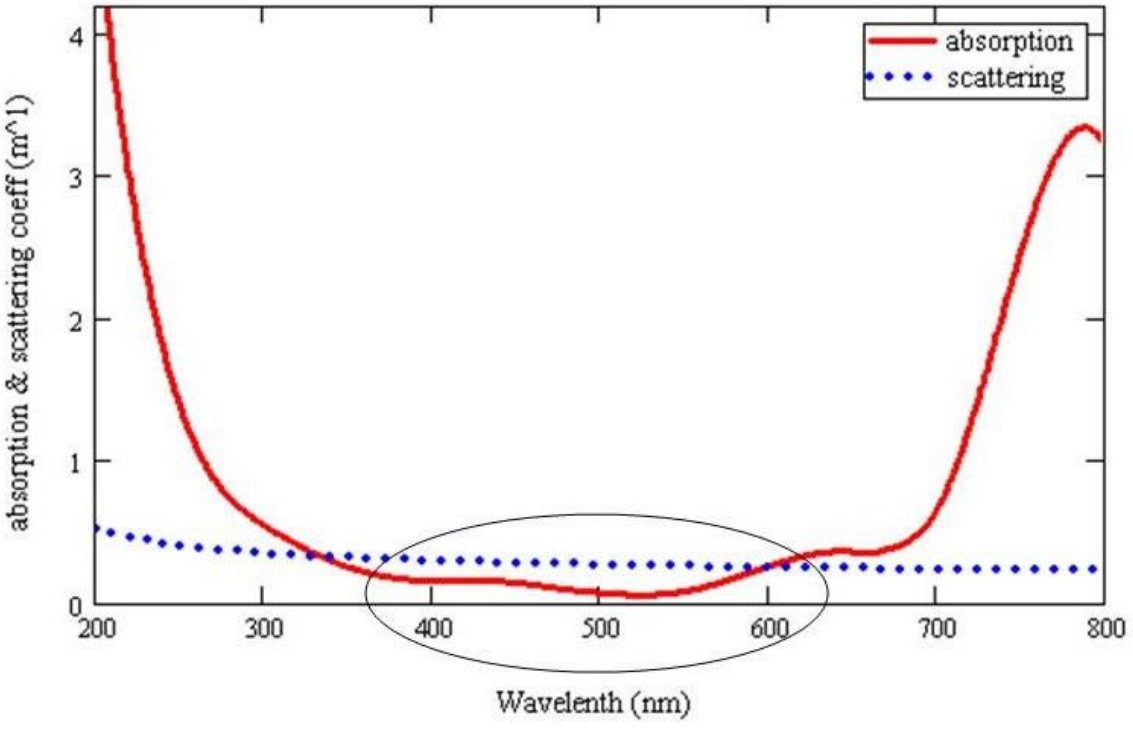

Fig. 1. Absorption and scattering coefficients of water with 1 mg/m^3 of chlorophyll concentration.

2. OPTICAL PROPERTIES OF WATER

When a photon is transmitted through a body of water, there are two mechanisms that prevent it from reaching a receiver further along the channel. The first of these is absorption, where the photon energy is converted into another form such as heat or chemical energy. The second is that a small variation in the refractive index causes the photon to change direction, this is known as scattering. The total attenuation loss coefficient, *c(λ)* is [12]:

$$c(\lambda) = \alpha(\lambda) + \beta(\lambda) \tag{1}$$

where *α(λ)* and *β(λ)* are absorption and scattering coefficients respectively, measured m^{-1} and λ is the wavelength of light in nm [13].

A. The absorption coefficient model

The form of absorption coefficient is a result of different biological factors; these factors include: the absorption of pure water and absorption by chlorophyll-a, which is the main substance that comprises phytoplankton, a group of photosynthesizing microorganisms, and absorption by humic and fulfic acids, both of which act as nutrients for phytoplankton. The full absorption spectrum coefficient is an addition of these spectrums multiplied by their respective concentrations such as [14]:

$$\alpha(\lambda) = a_w(\lambda) + a_c^0(\lambda).\left(\frac{C_0}{C_c^0}\right)^{0.602} + a_f^0 C_f \exp(-k_f.\lambda) + a_h^0 C_h \exp(-k_h.\lambda) \tag{2}$$

where $a_w(\lambda)$ is the pure water absorption coefficient which has value equal to 0.0257 m^{-1} for 500 nm; $a_c^0(\lambda)$ which is the spectral absorption coefficient of chlorophyll with values equal to 0.0125 m^{-1} for 500 nm [15, 16]; $a_f^0 = 35.959 m^2/mg$ and $a_h^0 = 18.828 m^2/mg$ are the specific absorption coefficient of fulfic acid and humic acid, respectively; C_f and C_h are the concentration of the fulfic acid and humic acid, correspondingly; while k_f and k_h are constants with values of 0.0189nm^{-1}, 0.01105nm^{-1} respectively. The concentrations of C_f and C_h are expressed through the chlorophyll concentration C_c as follows [14]:

$$C_f = 1.74098 C_c \exp\left[0.12327\left(\frac{C_c}{C_c^0}\right)\right] \tag{3}$$

$$C_h = 0.19334 C_c \exp\left[0.12343\left(\frac{C_c}{C_c^0}\right)\right] \tag{4}$$

where the constant with value equal to C_c^0 = 1 mg/m^3 and C_c is the total concentration of chlorophyll, which has different values depending on categories of Jerlov water types are shown in Table 1.

Table 1. Chlorophyll concentration for different Jerlov water types [4,17,18].

Jerlov Water Types	Concentration of Chlorophyll mg/m^3
I	0.03
IA	0.1
IB	0.4

B. The Scattering coefficient model

The mechanism of scattering process arises from pure water $\beta_w(\lambda)$, small particle $\beta_s^0(\lambda)$ and large particle $\beta_l^0(\lambda)$. Smalls particles have refractive index equal to 1.15, while large particles have a refractive index of 1.03 [19]. The scattering coefficient is expressed as [14]:

$$\beta(\lambda) = \beta_w(\lambda) + \beta_s^0(\lambda).C_s + \beta_l^0(\lambda).C_l \quad (5)$$

where C_s and C_l are the concentration of small and large particles, respectively, and $\beta_w(\lambda)$, $\beta_s^0(\lambda)$ and $\beta_l^0(\lambda)$ are the scattering coefficients by the pure water, small particles and large particles, given by [14]

$$\beta_w(\lambda) = 0.005826\left(\frac{0.4}{\lambda}\right)^{4.322}, m^{-1} \quad (6)$$

$$\beta_s^0(\lambda) = 1.151302\left(\frac{0.4}{\lambda}\right)^{1.7}, m^2/g \quad (7)$$

$$\beta_l^0(\lambda) = 0.3411\left(\frac{0.4}{\lambda}\right)^{0.3}, m^2/g \quad (8)$$

where C_s and C_l are the total concentration of small and large particles in g/m^3, respectively and can be expressed by:

$$C_S = 0.01739 C_C . \exp\left[0.11631 \left(\frac{C_C}{C_C^0} \right) \right], g / m^3 \quad (9)$$

$$C_l = 0.76284 C_C . \exp\left[0.03092 \left(\frac{C_C}{C_C^0} \right) \right], g / m^3 \quad (10)$$

3. ANALYSIS OF A LINK MODEL

i. Link Budget

To estimate of the received optical signal power P_r under line of sight (LOS) link as illustrated in Fig. (2) which is determined through empirical path loss models. The optical signal reaching the receiver is obtained by multiplying the transmitter power, telescope gain, and losses and is given by [19] as

$$P_r = P_T \eta_T \eta_R \exp\left[-c(\lambda) \frac{d}{\cos(\theta)} \right] . \frac{A_r \cos(\theta)}{2\pi d^2 \left[1 - \cos(\theta_0) \right]} \quad (11)$$

where P_t is the transmitted optical power, η_T and η_R are the optical efficiency of the T_x and R_x respectively, $c(\lambda)$ is the attenuation coefficient, d is the perpendicular distance between the T_x plane and R_x plane, θ_0 is the T_x beam divergence angle, θ is the angle between the perpendicular to the R_x plane and the T_x-R_x trajectory, and A_r is the receiver aperture area.

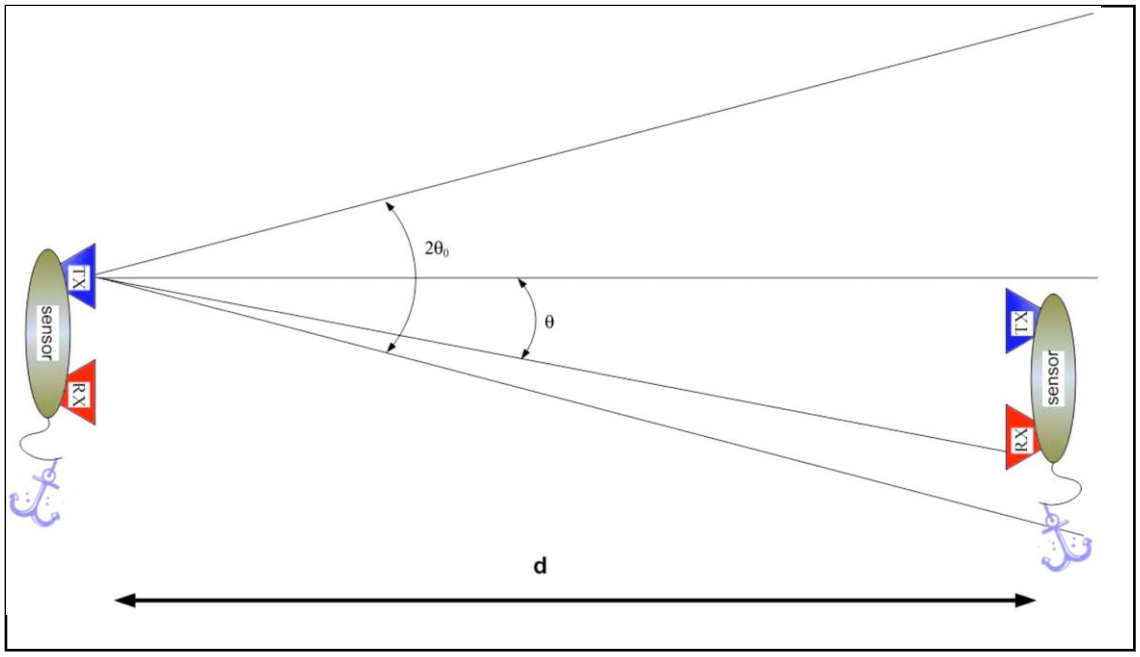

Fig. 2. Line- of- Sight (LOS) communication scenario.

ii. Detection of optical radiation

When transmitted optical signals arrive at the receiver, they are converted to electronic signals by photo detectors. There are many types of photo detectors in existence, photodiodes are used almost exclusively in optical communication applications because of their small size, suitable material, high sensitivity, and fast response time [20]. The types of photodiodes are the PIN photodiode and the avalanche photodiode (APD) which has good quantum efficiency and is made of semiconductors that are widely available commercially. For optimal design of the receiver system, it is important to understand the characteristics of these photodiodes and the noise associated with optical signal detection [21]. The performance of an APD is characterized by its responsivity $\Re_{APD}$. The average photocurrent generated by a steady photon stream of average optical power can be expressed as [22]:

$$I_p = \Re_{APD} P_r = M \Re P_r \tag{12}$$

where P_r is the average optical power received by the photo detector. The responsivity $\Re$ for Si, Ge and InGaAs APD is equal to 75 A/W, 35 A/W, 12 A/W respectively. The gain is designated by M, and is equal to 150, 50, and 20 for Si, Ge and InGaAs APD respectively [23]. The shot noise arises from the statistical nature of the production and collection of photoelectrons, for a photodiode the variance of the shot noise current I_{shot} in a bandwidth B_e is [20,22]:

$$< I_{shot}^2 >= \sigma_{shot}^2 = 2qI_p M^2 F(M) \tag{13}$$

where q is the electron charge and F(M) is the APD noise figure and is equal to 0.5, 0.95, 0.7 for Si, Ge and InGaAs APD [24]. The photodiode dark current arises from electrons and holes that are thermally generated at pn junction of the photodiode. If I_D is the dark current, then its variance is given by [20,22]:

$$< I_D^2 >= \sigma_D^2 = 2qI_D M^2 F(M) B_e \tag{14}$$

For Si, Ge and InGaAs APD the dark current I_D is 15nA, 700nA, 100nA respectively [23], and bandwidth B_e is equal to 5GHz, 0.2GHz and 2GHz for Si, Ge and InGaAs APD respectively [24]. On the other hand, the thermal noise arises from the random motion of electrons that is always present at any finite temperature, consider a resistor that has a value R at a temperature T. If $I_{thermal}$ is the thermal noise current associated with the resistor, then in a bandwidth B_e its variance $\sigma_{thermal}^2$ is [20,22]:

$$< I_{thermal}^2 >= \sigma_{thermal}^2 = \frac{4k_B T}{R} B_e \tag{15}$$

The total noise current $< I_N^2 >$ can be written as [20,22]

$$< I_N^2 >=< I_{shot}^2 > + < I_D^2 > + < I_{thermal}^2 > \quad (16)$$

The signal to noise ratio is given by [20,22]

$$SNR = \frac{< I_P^2 M^2 >}{< I_N^2 >} = \frac{I_p^2 M^2}{2q(I_p + I_D)M^2 F(M) B_e + 4k_B T B_e / R} \quad (17)$$

iii. Bit Error Rate (BER) for underwater communications

BER is defined as the probability of code errors during transmission [25]. The relation between BER and the signal to noise ratio SNR is as follows [21,26]:

$$BER_{L-PPM} = \frac{1}{2} erfc\left(\frac{1}{2\sqrt{2}} \sqrt{SNR \frac{L}{2} \log_2 L}\right) \quad (18)$$

where L is the pulse position code.

iv. Channel capacity

The channel capacity (C_s) is defined as a maximum rate of information data stream within the communication channel. The maximum rate of 1 bit per channel use can be achieved, but only when the SNR is infinite. The capacity of the channel gives a theoretical limit for the transmission rate of (reliable, i.e., error-free) data from a transmitter of given power, over channel with a given bandwidth, operating in a given noise environment [27]. The channel capacity per symbol is given by [28]

$$C_S = 1 + BER \log_2 BER + (1 - BER) \log_2 (1 - BER) \quad (19)$$

4. NUMERICAL RESULTS

Table 2. System parameters used in the simulation [14,26,27]

Parameter	Value
Transmission Wavelength (λ)	500 nm
Transmitter power (P_T)	50 mw
Optical efficiency of transmitter η_T	0.9

Optical efficiency of receiver η_R	0.9
Laser beam divergence angle (θ_0)	60°
Transmitter inclination angle (θ)	(1°, 5°)
Receiver aperture area (A)	0.01 m^2
Electron charge (q)	1.6×10^{-19} C
APD load resistance (R)	(10,100) Ω
Boltzmann constant (k_B)	1.38×10^{-23} J·K
Temperature (T)	298 K

In this section, using the above mentioned formulations, the simulation is carried out to study the underwater optical channel and its effect on optical wireless communication employing M-PPM modulation technique in the transmitter and different APD receiver in underwater environment. The values of the simulation parameters and constants are given in Table (2).

A. Received signal power as a function of distance

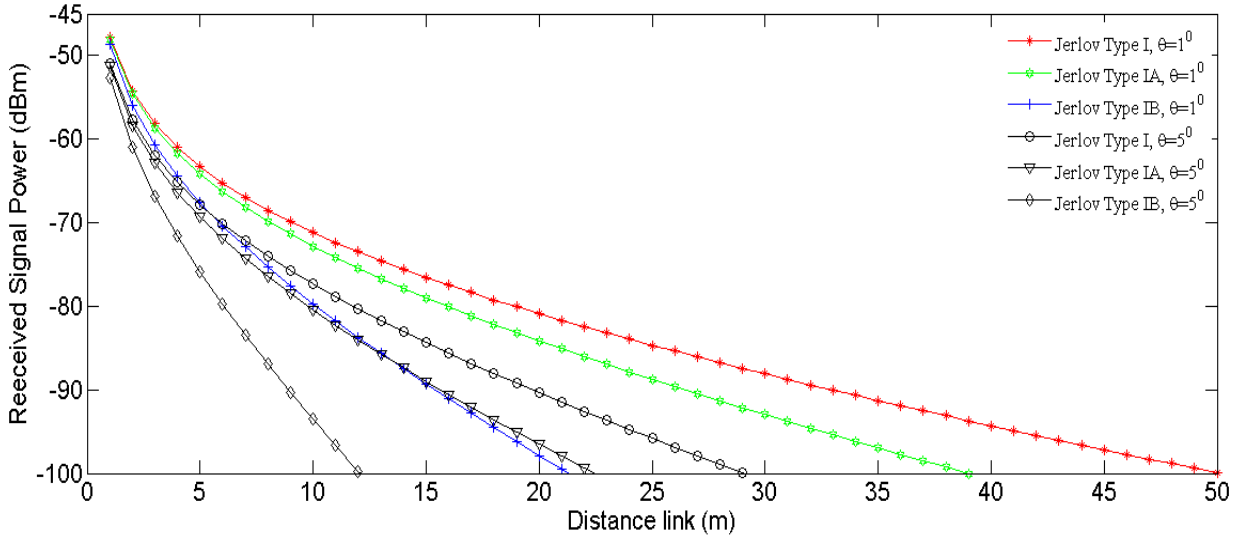

Fig. 3. Receiver signal power for an underwater environment

In an underwater optical wireless communication system, communication distance is an important indicator. It is meaningful to study achievable distance d of optical beam under

different water mediums. Let us see the effect of the total attenuation coefficient $c(\lambda)$ on the received optical power P_r based on line of sight model (LOS) for optical beam propagation horizontally in an underwater medium. It is shown in Fig. (3) P_r as the function of distance d for transmitter inclination angle θ (1°, 5°) under three Jerlov water types specified in table 1. In this case, the wavelength λ = 500 nm is used. Suppose to be the case a tolerable loss is of − 100 dBm beyond which the signal is not detectable at the receiver. It is noticed that, for transmitter inclination angle θ = 5°, the transmission range is limited to 12 m, 23 m and 29 m for Jerlov type IB, IA, and I waters respectively. When the transmitter inclination angle decreases θ = 1°, Jerlov type I increases dramatically a range exceed 50 m and reach to 39 m, 22 m for IA, IB water respectively. There is factual increase in achievable transmission distance when the chlorophyll concentration decreases. It can be conclude that when a water quality is good, improvement increase occurs in achievable transmission distance significantly.

B. BER characteristics for underwater optical wireless communications

BER plays a crucial role in an optical communication system. We present here simulation results to compare the performance of APDs detectors under different Jerlov water types. On the other hand, we consider 4-PPM modulation technique on the transmitter side:

1. The impact of the distance of transmission

Let us consider the BER performance as a function of the distance of transmission. Fig. (4) shows the curves of the BER for different APD detectors under jerlov water type I, IA, and IB when a transmitter inclination angle of θ =1° is used. In this case, it is noticed that for BER 10^{-10}, the distance transmission is limited to 7 m, 10 m and 12 m for Jerlov IB, IA and I respectively when an InGaAs is used as a detector. For Ge the distance is about 13.5 m for IB detector, and it increases for IA, it becomes about 23.5 m. It is noticed that for I water applied as a channel the distance of transmission reaches to 27 m. An improvement increase occurs when we Si is used as a detector, where the distance of data transmission increases and reaches 24 m and 29 m for IB and I water. In Fig. (5) it is assumed that the underwater optical wireless communication operates in θ = 5° condition. It is clear that the BER curves for the modulation technique decreases with increase in the distance of transmission. In this case, the data of the transmission does not exceed 16 m, 17 m for Ge, Si detectors respectively under Jerlov water I. This decrease in distance of data transmission comes from increase in chlorophyll concentration.

Another important simulation to evaluate the performance of BER for APDs is on the receiver side. It is noticed in Fig. (6) a significant increase in the distance of transmission which can be achieved by using the resistance load (R)100 Ω, the maximum data transmission is about 31 m, 34m for Ge, Si detectors respectively for jerlov type I. On the other hand, the distance of the data transmission decreases for the other Jerlov water types. The receiver sensitivity of InGaAs is lower than that of the other detectors, therefore the BER performance of InGaAs is poor. When we applied a θ = 5° condition is applied to a transmitter inclination angle as shown in Fig. (7), it is clear that the BER curves decrease with increase in transmitter inclination angle and distance link. The maximum data transmission reach to 19 m, 20 m for detectors Ge, Si respectively under jerlov type I. Notice that in jerlov water type I as a communication medium, an approximate by 2 dBm occurs in the BER performance for Si and Ge APD.

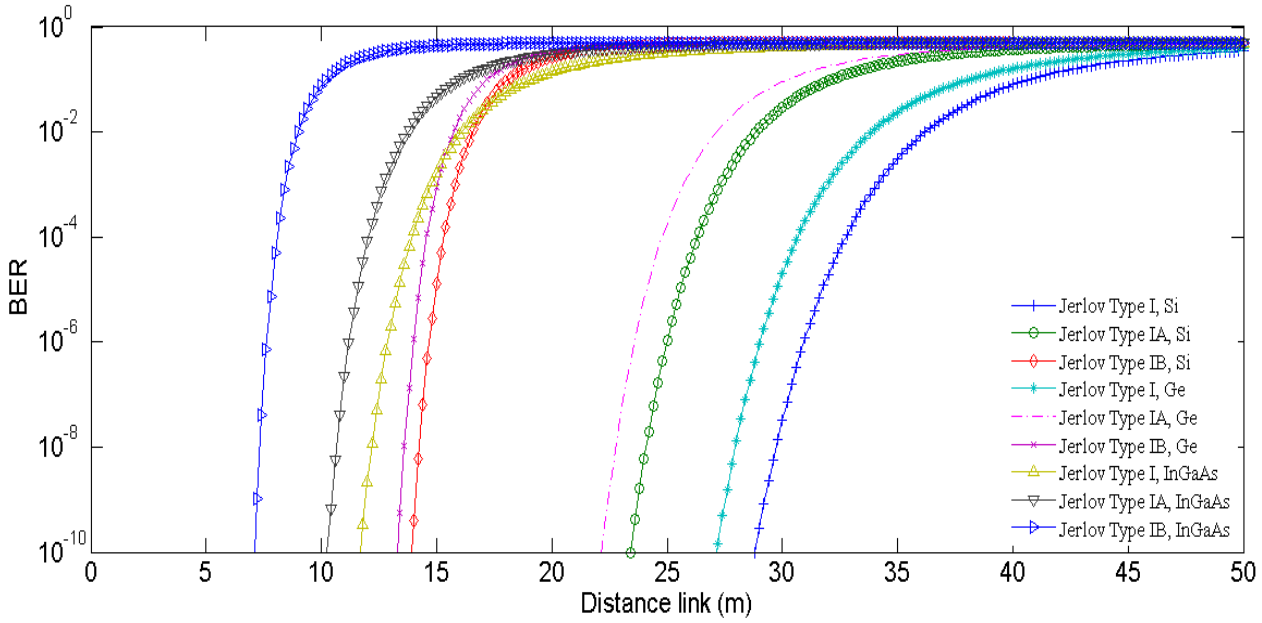

Fig. 4. BER versus distance link (m) when θ = 1°, R = 10 Ω and Pt = 50 mw

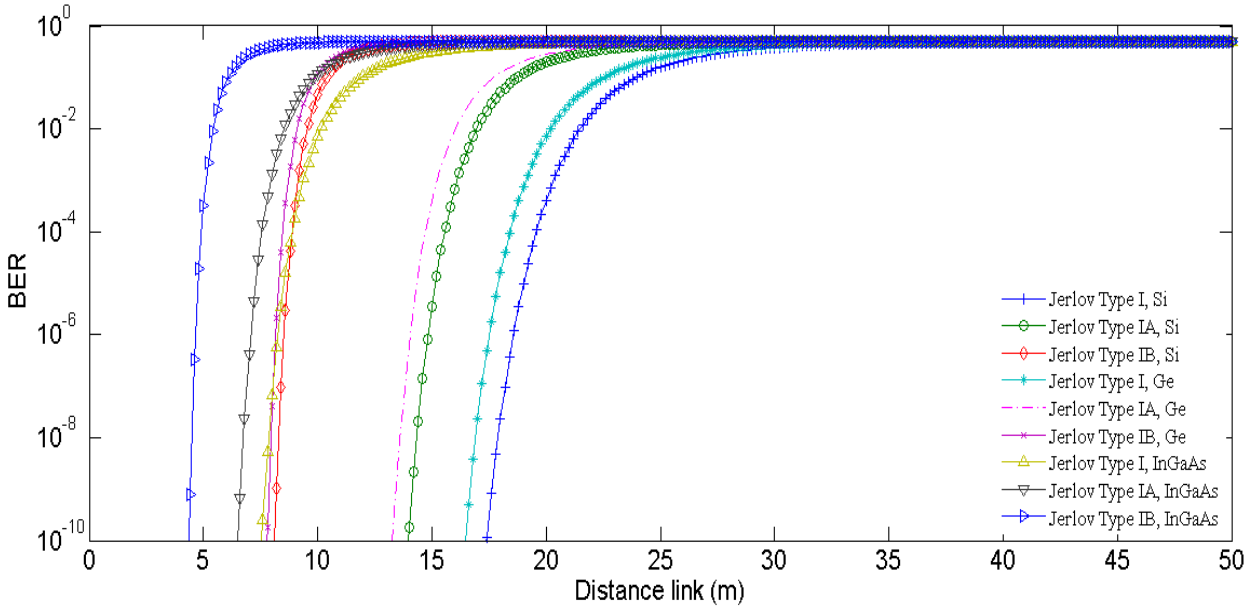

Fig. 5. BER versus distance link (m) when θ = 5°, R= 10 Ω and Pt = 50 mw

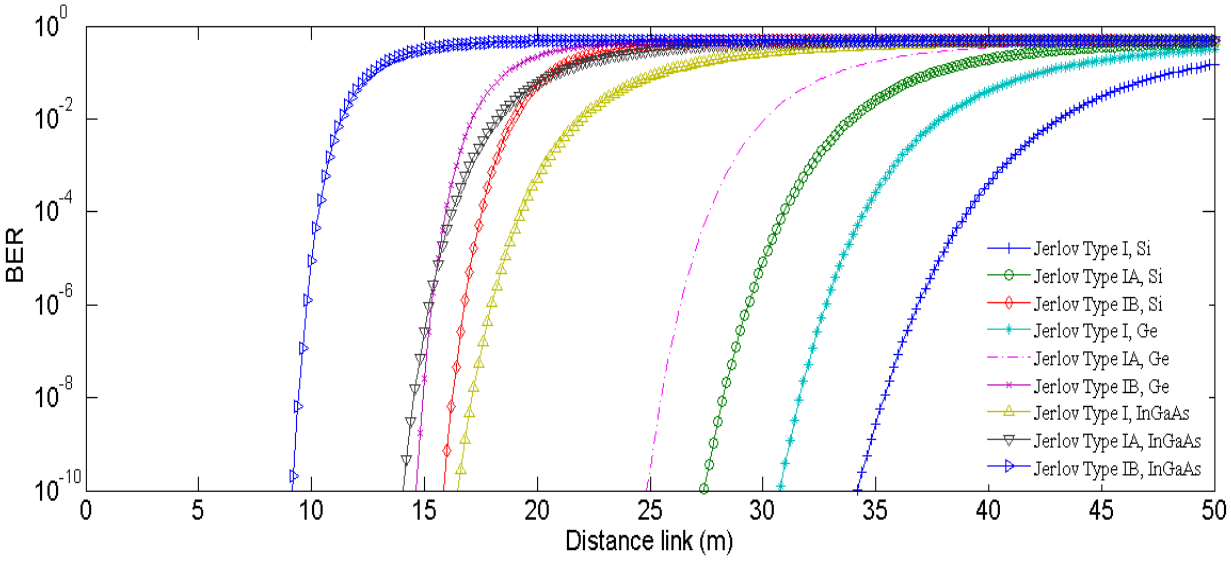

Fig. 6. BER versus distance link (m) when θ = 1°, R = 100 Ω and Pt = 50 mw

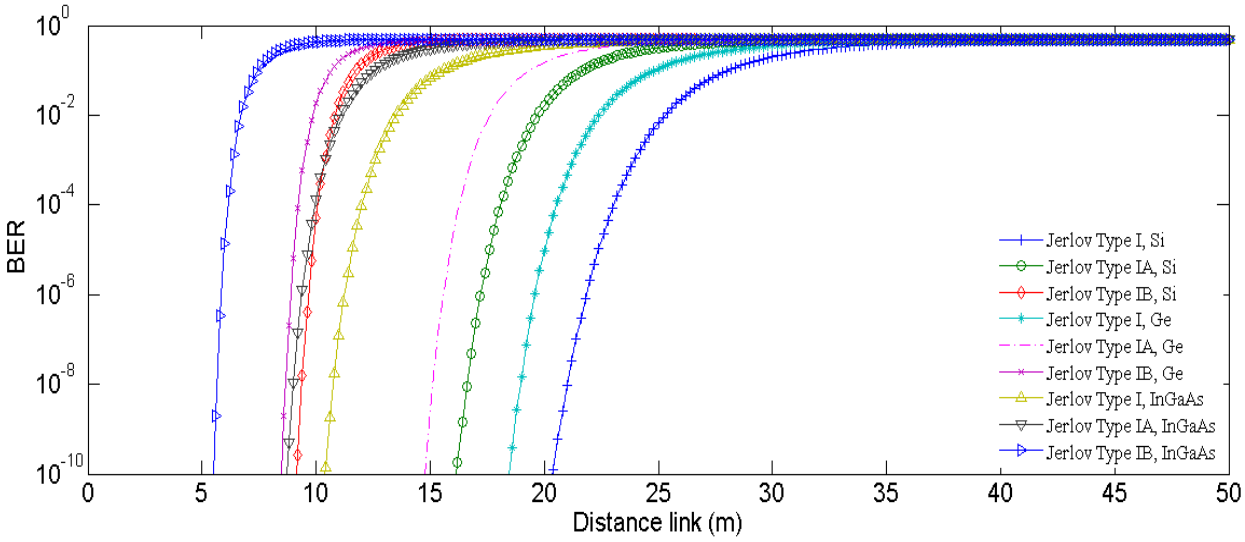

Fig. 7. BER versus distance link (m) when θ = 5°, R = 100 Ω and Pt = 50 mw

2. The impact of the power of transmitter

It is investigated the effect of power transmitter on BER under transmitter inclination angle θ = 1°. We compare the performance of APDs detectors when a 4-PPM is used as a modulation technique with different Jerlov water types. Fig. (8) shows the BER versus the power of the transmitter when the distance of transmission d = 35 m. If we consider a required BER 10^{-10}, when we use a Jerlov type I as a communication channel, the power of transmitter

is about -21 dBm for Si APD and -19 dBm for Ge APD. When the resistance load is increased, as is evident in Fig. (9), the underwater optical communication system depends on the resistance load. As an increase in the resistance load (R = 100 Ω) leads to a decrease in the required power of transmission reaching to more than -30 dBm, -22 dBm for Si, Ge APDs respectively for a Jerlov type I and BER of 10^{-10}. On the other hand, when we apply InGaAs as a detector the power of transmitter would be about 11 dBm for Jerlov type I. The receiver sensitivity decreases when the attenuation of water is increasing.

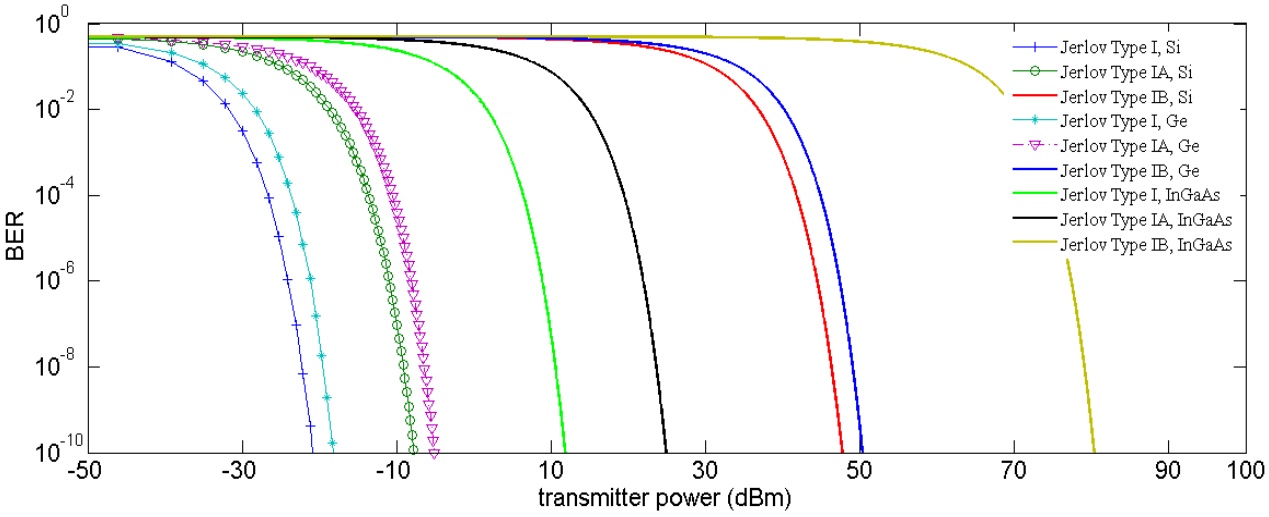

Fig. 8. BER versus transmitter power (dBm) when θ = 1°, R = 10 Ω and d = 35m

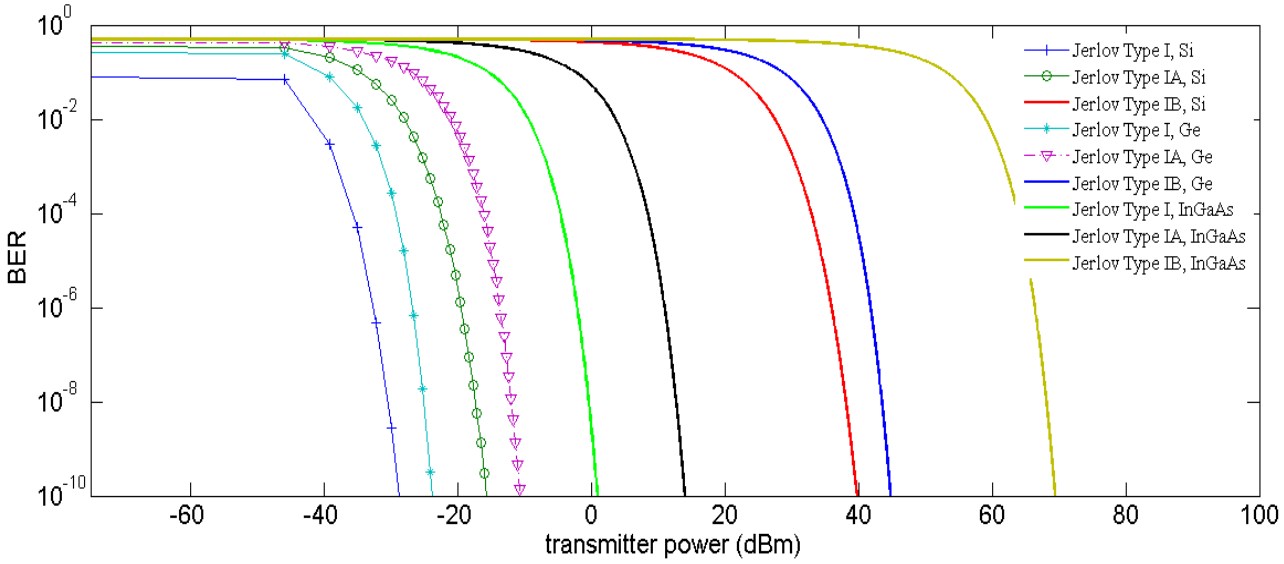

Fig. 9. BER versus transmitter power (dBm) when θ = 1°, R = 100 Ω and d = 35 m

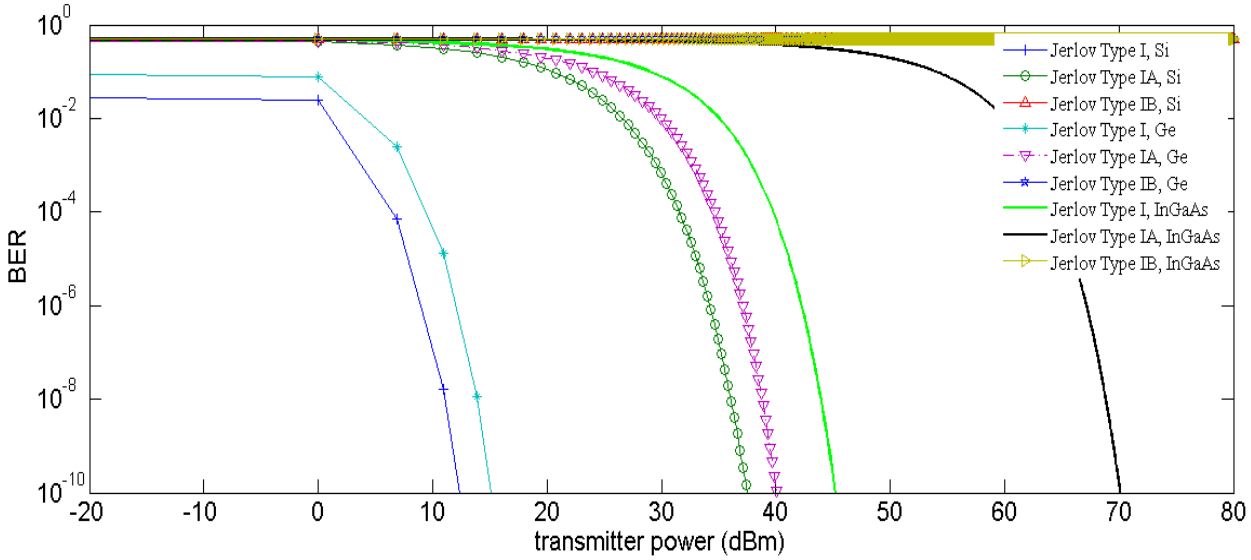

Fig. 10. BER versus transmitter power (dBm) when θ = 5°, R = 10 Ω and d = 35m

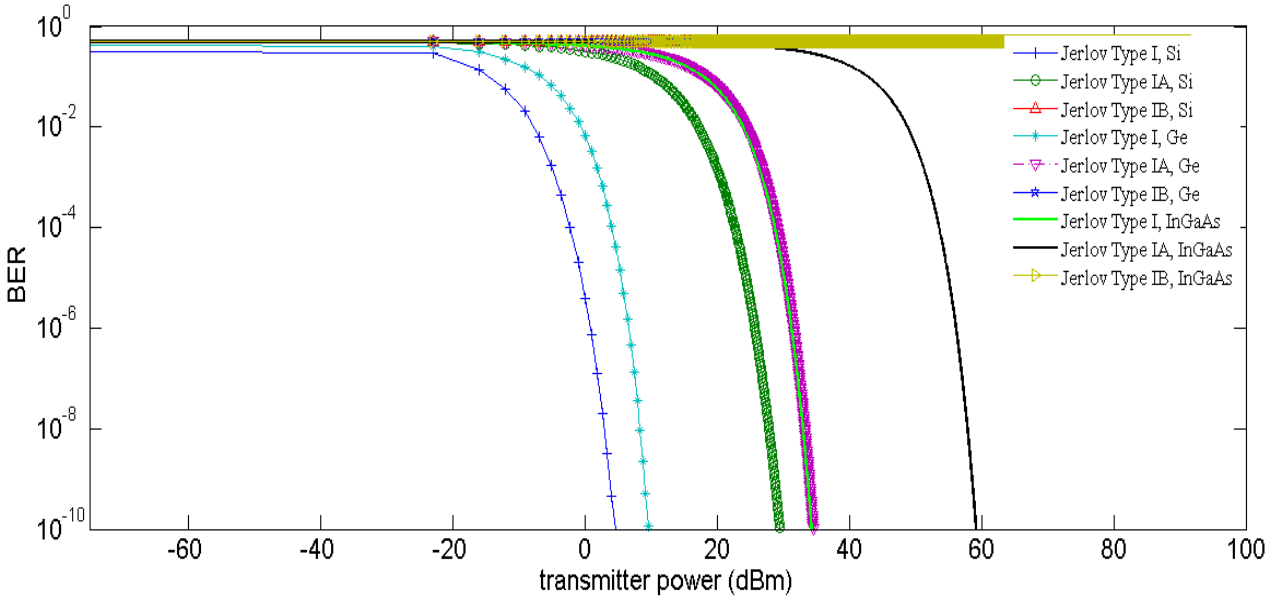

Fig. 11. BER versus transmitter power (dBm) when θ = 5°, R = 100 Ω and d = 35m

We performed the same calculations also on transmitter inclination angle θ = 5° under Jerlov types I, IA and IB as a communication medium. Fig. (10) shows BER for resistance load R = 10 Ω. For a target of BER of 10^{-10}, the power of transmitter was about 12 dBm, 15 dBm for Si, Ge APDs respectively, while InGaAs detector has not sensitivity under the same conditions. This behavior of the curves leads to increase in the required power of the

transmitter when Jerlov types IA, IB are applied. An analogous situation is given in Fig. (11), when a resistance load R = 100 Ω is applied. If we consider a required BER of 10^{-10}, the power of transmitter reaches to 5 dBm, 10 dBm for Si. Ge APDs respectively. It is concluded that when a transmitter inclination angle is increased the required power of transmitter is increases.

C. Channel capacity

The channel capacity is presented in terms of BER of underwater optical wireless communication, under Jerlov water types as a communication channel for various values θ of 4-PPM modulation technique as shown in Fig. (12, 13). In Fig. (12), when θ = 1°, it is inferred that the information data increases along with distance decrease. The channel capacity can reach maximum value of 1 when Jerlov type I and Si APD are applied. Fig (13) shows channel capacity against distance link when θ = 5°. It is intuitively clear that the increase in transmitter inclination angle leads to a reduction in the channel capacity.

Fig. (14 and 15) show channel capacity as a function of transmitter power for d=35m considering different water types and different APD detectors. When the transmitter inclination angle is θ = 1° as shown in Fig. (14), if we consider a maximum channel capacity 1, this value leads to a Jerlov type I as a communication channel for Si APD the power of transmitter is about -50 dBm. When a transmitter inclination angle is increasing, as is evident in Fig. (15), the transmitter inclination angle (θ = 5°) increases of the required power of transmission reached to -20 dBm. On the other hand, when we applied InGaAs as a detector the power of transmitter would be about 20 dBm for Jerlov type I. For Jelov type IB the receiver sensitivity is very poor.

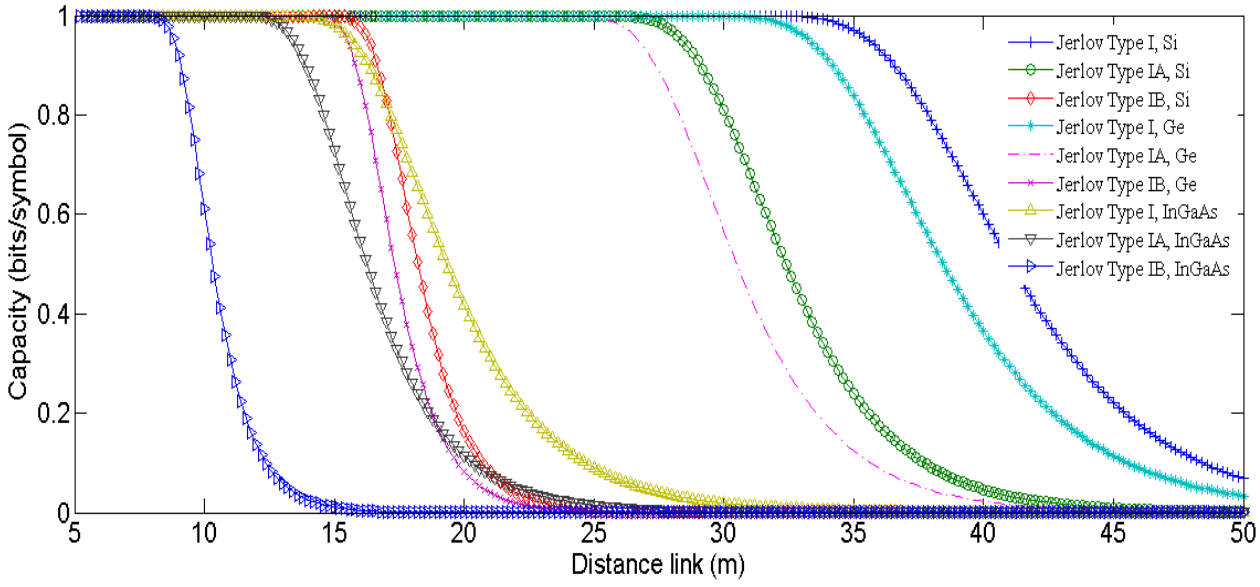

Fig. 12. Channel Capacity versus distance link (m) when θ = 1°, R = 10 Ω and Pt = 50 mw

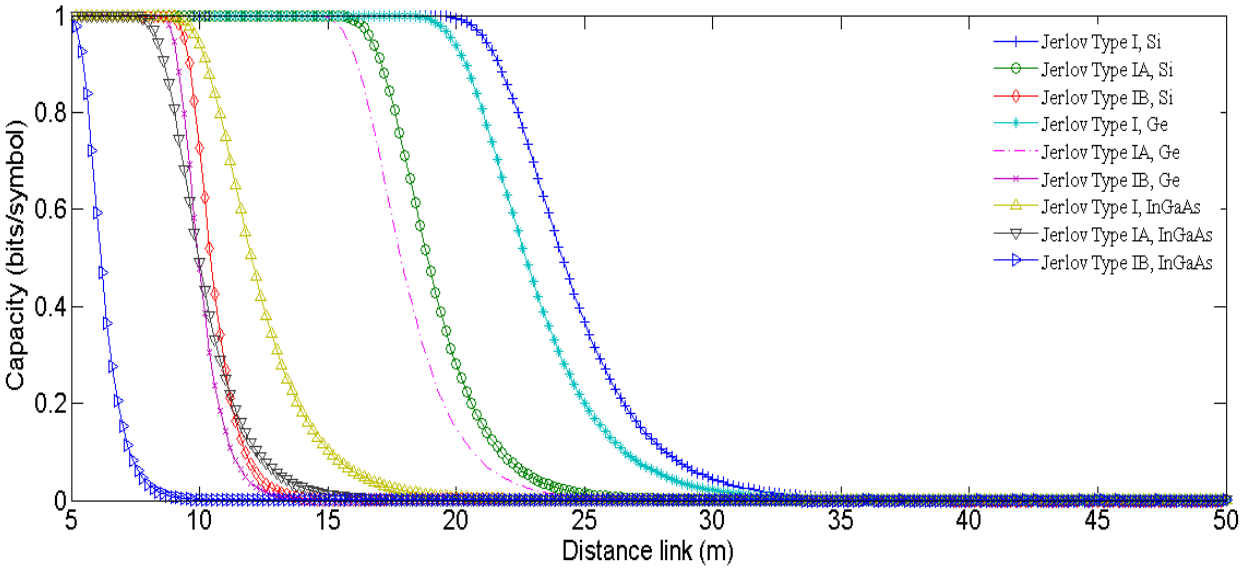

Fig. 13. Channel Capacity versus distance link (m) when θ = 5°, R = 10 Ω and Pt = 50 mw

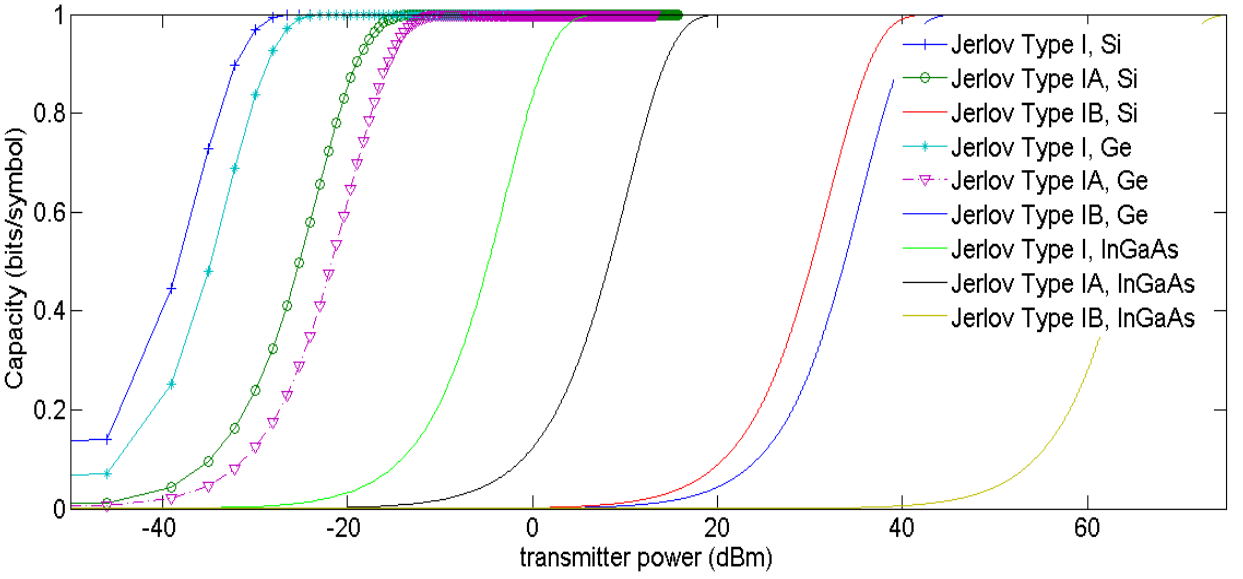

Fig. 14. Channel Capacity versus transmitter power (dBm) when θ = 1^0, R = 10 Ω and d = 35 m

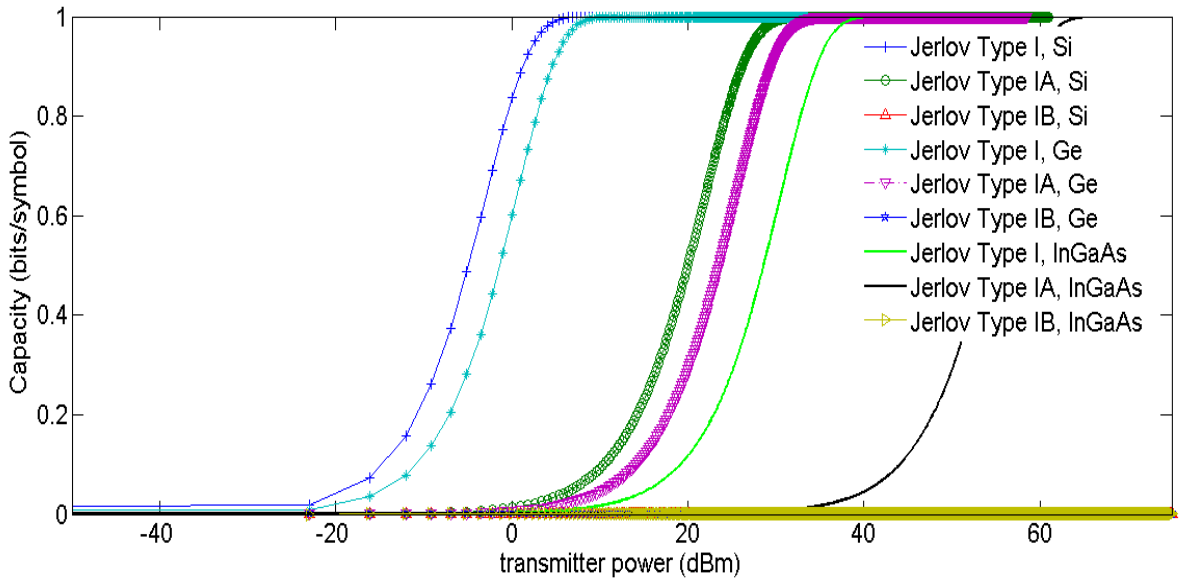

Fig. 15. Channel Capacity versus transmitter power (dBm) when θ = 5°, R = 10 Ω and d = 35 m

5. CONCLUSIONS

This paper provides a theoretical performance analysis of an underwater optical wireless communication link using 4-PPM modulation technique in the transmitter and different an APD as a receiver with precisely aligned LOS geometry model for Jerlov water types (I, IA, IB).

The attenuation coefficient of laser beam through an underwater environment has a significant effect on the performance of underwater communication systems. The effect of chlorophyll concentration, distance of communication, transmitter inclination angle and resistance load are investigated.

The suitable choice of wavelength has a strong influence on the received optical power and SNR which leads to long transmission in water. When water has increasing in chlorophyll concentration, this causes a decrease in received optical power, where Si, Ge and InGaAs APD are employed in the receiver side.

The BER characteristics of the 4-PPM modulation technique under different Jerlov water types and APD detectors are studied. The results show that the Si APD detector has a greater advantages than the others for Jerlov type I. therefore, a Si APD is a more suitable receiver compared with Ge APD.

When a transmitter inclination angle (θ = 5°) and a Jerlov types is IA, IB is applied as a communication medium, the BER for a Si APD has the analogous behavior to the Ge, InGaAs APD. We compare the performance of BER, channel capacity when an APD used as a detector with link distance 35 m.

References

[1] A. Choudhary, V. K. Jagadeesh, P. Muthuchidambaranathan, "Pathloss analysis of NLOS underwater wireless optical communication channel", International conference on electronic and communication system (ICECS), India, 2014.

[2] L. Mullen, A. Laux, B. Cochenour, "Propagation of modulated light in water: implications for imaging and communications systems", *Applied optics*, vol. 48, no.4, 2009.

[3] M. A. Khalighi, C. Gabriel, T. Hamza, S. Bourennane, P. Léon, and V. Rigaud, "Underwater Wireless Optical Communication; Recent Advances and Remaining Challenges", International Conference on Transparent Optical Networks (ICTON), Austria, 2014.

[4] Y. J. Gawdi, "Underwater Free Space Optics, "M.S. thesis, North Carolina State University, Raleigh, NC, (2006).

[5] S. Tang, X. Zhang, Y. Dong, "On impulse response for underwater wireless optical links" IEEE oceans conferences-Bergen, MTS/IEEE, (2013).

[6] C. Gabriel, M.A. Khalighi, S. Bourennane, P. Léon, V. Rigaud, "Monte-Carlo-Based Channel Characterization for Underwater Optical Communication Systems," IEEE/OSA *Journal of Optical Communications and Networking* (JOCN), vol.5, no.1, pp. 1-12, 2013.

[7] S. Tang, Y. Dong, X. Zhang, "On link misalignment for underwater wireless optical communications", *IEEE Communication Letters*, vol. 16, no. 10, pp. 1688-1690, 2012.

[8] S. Vigneshwaran, I. Muthumani, & R. A. Sivananantha, "Investigations on Free space optics communication system", International Conference on Information Communication & Embedded Systems (ICICES), India, 2013.

[9] M. T. Rahman, S. Iqbal, & M. M. Islam, "Modeling and performance analysis of free space optical communication system", International Conference on Informatics, Electronics & Vision (ICIEV), 2012.

[10] S. A. Al-Gailani, A.B. Mohammad & R. Q. Shaddad, "Enhancement of free space optical link in heavy rain attenuation using multiple beam concept", *Optik*, vol. 124, iss. 21, pp. 4798-4801, 2013.

[11] M. Ijaz, Z. Ghassemlooy, S. Rajbhandari, H. Le Minh, J. Perez, & A. Gholami, "Comparison of 830 nm and 1550 nm based free space optical communications link under controlled fog conditions", 8th International Symposium on Communication systems, Networks and Digital Signal Processing (CSNDSP), 2012.

[12] N. G. Jerlov, "Marine optics", *Elsevier science*, (1976) 13-63.

[13] L. J. Johnson, R. G. Green, M. S. Leeson, "Underwater optical wireless communications: depth dependent variations in attenuation", *Applied Optics*, vol.52, no. 33, 2013.

[14] V. I. Haltrin, "Chlorophyll-based model of sea water optical properties", *Applied Optics*, 38 (1999) 6826-6832.

[15] V. I. Haltrin, G. W. Kattawar, "Effect of Raman scattering and fluorescence apparent optical properties of sea water", Texas A&M University, (1991).

[16] R. C. Smith, K. S. Baker, "Optical properties of the clearest natural waters", *Applied Optics*, 20 (1981) 177-184.

[17] J. R. Apel, "Principles of ocean physics", London, Academic Press Inc, pp. 580-585, 1987.

[18] C. D. Mobley, D. Stramski, P. W. Bissett, and E. Boss, "Optical modeling of ocean water", *Oceanography*, vol. 17, (2004).

[19] S. Arnon, D. Kedar, "Non-Line-of-sight underwater optical wireless communication network", *J. Opt. Soc. Am. A*, vol. 28, 3 (2009).

[20] G. Keiser, "Optical fiber communications", McGraw-Hill Company, (2000).

[21] S. Trisno, "Design and analysis of advanced free space optical communication systems", Ph. d thesis, University of Maryland, (2006).

[22] G. Keiser, "Optical essential communications", McGraw-Hill Company, (2004).

[23] K. C. Palais, "Fiber optic communications", Prentice-Hall Inc, 4th edition, 2004.

[24] Z. Ghassemlooy, W. Popoola, S. Rajbhandari, "Optical wireless communications system and channel modeling with matlab", CRC press, Taylor & Frances Group, 2013.

[25] Y. Ding, Q. Ding, Q. Liu, "Performance Analysis of optical modulation in underwater slant transmission", *International journal of innovative computing, information and contron*, vol. 9, no. 9, pp. 3799-3805, 2013.

[26] W. O. Popoola, Z. Ghassemlooy, "BPSK subcarrier intensity modulated free-space optical communications in atmospheric turbulence", *Journal of Lightwave technology*, vol. 27, no. 8, pp. 967-973, 2009.

[27] A. Majumdar, "Advanced Free Space Optics (FSO) a systems approach", Springer Science+Business Media New York, 2015.

[28] D. A. Luong, T. C. Thang, A. T. Pham, "Effect of avalanche photodiode and thermal noises on the performance of binary phase-shift keying-subcarrier-intensity modulation/free-space optical systems over turbulence channels", *IET Communications*, vol. 7, iss. 8, pp. 738-744, 2013.

(Received 19 March 2016; accepted 03 April 2016)